CONFIDENTIAL

Evaluation of Electrical Power Generation by BlackLight Power's High-Power-Density Catalyst Induced Hydrino Transition (CIHT) Cells

Report Submitted
to

BlackLight Power, Inc
493 Old Trenton Road, Cranbury, NJ 08512

By

Dr. Terry Copeland
at
The ENSER Corporation
5430 70th Ave North, Pinellas Park, FL 33781

Dated 15th December 2012

Background

Dr. Randell Mills of BlackLight Power, Inc. (BLP) has developed the "Grand Unified Theory of Classical Physics," by the application of physical laws and first principles rather than pure mathematics[1]. Based on this theory, Dr Mills has calculated, with great precision, bond energies and molecular structures that have been verified through experimental observation and reported in the literature. The theory predicts that there is a more stable lower energy state of hydrogen than previously believed. He has identified this more stable state of hydrogen as the "hydrino." Mills theory predicts that the transition of H to a stable hydrino state $H\left[\frac{a_H}{p=m+1}\right]$ having a binding energy of $p^2 \cdot 13.6\ eV$ occurs by a nonradiative resonance energy transfer of $m \cdot 27.2\ eV$ (m is an integer) to a matched energy acceptor such as nascent H_2O that has a potential energy of 81.6 eV (m = 3). The nascent H_2O molecule formed by an oxidation reaction of OH^- at a hydrogen anode is predicted to serve as a catalyst to form $H(1/4)$ with an energy release of 204 eV compared to the 1.48 eV required to produce H from electrolysis of H_2O. A transition from hydrogen in the traditional molecular state, H_2, to the hydrino state will release energy up to two hundred times greater than combusting the same amount of hydrogen. BLP has invented an electrochemical cell, the catalyst induced hydrino transition cell (CIHT), to harness this energy as direct electrical output. The CIHT cell contains an anode, unique electrolyte and a cathode as indicated in the schematic below. Atomic hydrogen is formed via initial electrolysis of water vapor flowing into the cell. That hydrogen is then converted via catalytic reaction of the unique electrolyte to form hydrinos. The energy released by the formation of hydrinos is captured as net electrical output of the CIHT.

[1] R. Mills, *The Grand Unified Theory of Classical Physics*, July 2010 edition, http://www.blacklightpower.com/theory/bookdownload.shtml.

CIHT cell schematic:

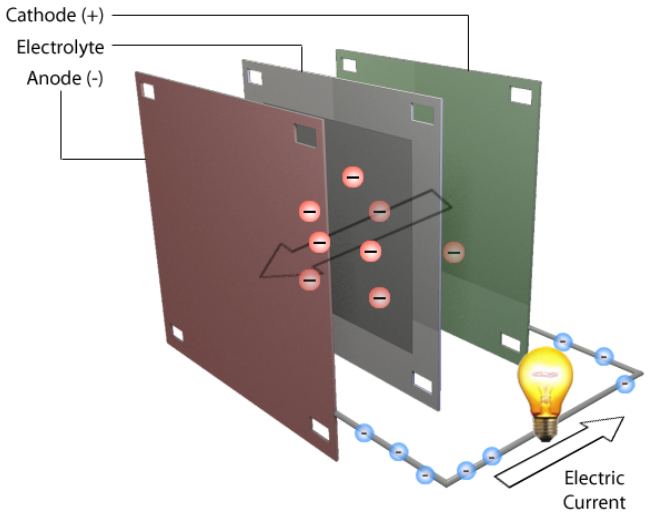

As reported in my May 28, 2012 validation study, on November 30th, I witnessed careful assembly of three closed CIHT cells supplied with H_2O vapor entrained in an inert (argon) carrier gas as the only mass input. The cells were run under an intermittent electrolysis condition to provide hydrogen at the anode and oxygen at the cathode. One test cell was comprised of a pre-oxidized porous nickel cathode, LiOH-LiBr-MgO electrolyte, and a pressed porous nickel anode. Two other test cells used a molybdenum (Mo) anode or a Mo alloy (Haynes 242). The startup of the cells and data collection setup was also witnessed. Initial data indicated that all three cells showed excess energy production during discharge compared to the energy input during short charge pulses. The Mo anode cell showed much higher energy discharge excess than the nickel anode cell. The alloy 242 was intermediate. Periodic updates of the data were sent by BLP staff. I returned to BLP on December 15th, 2011. At that time the accumulated electrical energy gain from these cells were 207% (Ni), 547% (Haynes 242), and 5476% (Mo). These cells ran for a total of three weeks with stable performance, at which point they were shut down so that other experiments could be run.

No readily recognized reaction is expected to occur at the electrodes or the electrolyte that could produce the observed electrical energy. Furthermore, there is no possible reaction of H_2O with the cell constituents based on system thermodynamics. Dr. Mills' theory offers a plausible explanation: H formed during electrolysis undergoes a reaction to form hydrinos with the release of electrical energy. Results were consistent with the proposed CIHT cell half-cell reactions forming the hydrino catalyst in the presence of atomic hydrogen, and the cell

performance matched predictions based on the hydrino mechanism including the upfield NMR results characteristic of the hydrino product. Albeit these first generation CIHT cells served as a proof of principle of the breakthrough new source of electricity, the power density was low, about 0.2 mW/cm^2 and correspondingly, the cell power was low, about 2-3 mW.

This present validation program was completed through off-site tests conducted on CIHT cells at the Enser Corporation's Tampa FL facility. CIHT cells, each comprising a Mo or MoCu (50-50 at%) foil or Mo or MoCu (50-50 at%) hydrogen permeable membrane anode, NiO cathode, and a LiOH-LiBr eutectic mixture as the electrolyte were tested for hydrino formation as a half-cell reaction to serve as a new electrical energy source. The power density was increased by a factor of up to 500 times that of the prior CIHT cells. The cells were operated under intermittent H_2O electrolysis to generate hydrogen at the anode and oxygen at the cathode then discharged to form hydrinos wherein H_2O vapor as well as some O_2 was supplied from the atmosphere in open cells. Net electrical production over the electrolysis input and hydrogen supplied to the anode was measured using an Arbin BT 2000 (<0.1% error) and confirmed using a digital oscilloscope. A possible anode-air reaction was tested by measuring the thickness of the anodes before and after operation as well as by comparison to a control electrolyte that was capable of a greater rate of metal oxidation but did not produce excess electrical energy. Characteristic signatures of the hydrino products were sought using three analytical techniques.

Dr. James Pugh (electrolyte scientist and Director of Technology at ENSER) and Dr. Ethirajulu Dayalan (electrochemist and Research Fellow at ENSER) participated with me in the independent tests of CIHT cells at Enser's Tampa FL facility starting on November 28, 2012– the purpose of which was to determine whether BlackLight had achieved high power density with stabilization of the anode from corrosion by maintaining a negative operating voltage relative to the thermodynamic anode corrosion voltage and by the presence of hydrogen supplied to the anode through the hydrogen permeable membrane. The second purpose was to determine if hydrino was the product of any excess electricity observed. The third purpose was to independently validate BlackLight's results off-site by an unrelated highly qualified party.

CIHT Cell Electrical Energy Balance. An exemplary CIHT cell comprised (i) a 6.5 cm ID X 14 cm IH alumina crucible containing the cell components, (ii) (a) MoCu (50-50 at%, AMETEK) hydrogen permeable anode comprising a diaphragm made of two pieces of 1.5" OD 0.040" and 0.020" thickness foils welded together and joined to a 3/8" OD or 1/4" OD Ni H_2 supply tube, respectively. The hydrogen was supplied from a two liter tank having a H_2 pressure in the range of 950 ± 30 Torr monitored using a Baratron gauge; (b) Mo foil anode, 1 X 1 cm, $1cm^2$, and (iii) a molten eutectic salt electrolyte comprising LiOH (15 g)-LiBr (75 g). The electrode spacing was 0.2-0.3 cm maintained by an alumina separator ring. The alumina crucible containing the cell components was placed in a resistive heater that maintained the temperature

of the electrolyte at 430 ± 2 °C. The cell was operated open to atmosphere. Control cells of the anode metal-air reaction as a source of electricity comprised identical cells with the LiOH-LiBr electrolyte replaced by KOH (61.8 g) -KBr (51 g) that has a much higher oxygen reduction rate and is predicted to be a superior electrolyte for any possible metal-air contribution to the energy balance.

Nickel leads from the anode and stainless steel leads from the cathode were attached to the leads of a recently calibrated Arbin BT2000 fuel cell and battery testing system. The cell was run under intermittent electrolysis conditions. The programmed waveform comprised the steps of (i) charge at constant current such as 50 mA for 1s duration and (ii) discharge at 50 mA constant current for 2s duration. The Arbin BT2000 voltage, current, and power waveforms and energy were confirmed with a digital oscilloscope. An occassional anomoly was observed wherein the charge/discharge cycle was ~50% longer than programmed, but in all cases the discharge cycle appeared longer than the charge cycle. The anomoly apparently was a result of the CPU load on the Arbin controlling computer. This typically occurs when a resource intensive load is being placed on the Arbin controlling computer that is outside of the Arbin controlling software – for instance, loading results data for an Arbin experiment in Excel or Data-watcher, which was being done. When it occurs the waveform is temporarily skewed for a few seconds as the computer diverts resources to tasks other than running the real-time Arbin schedule, and the waveform then returns to the programmed schedule as soon as CPU resources return to the Arbin software and the CPU is back to steady state.

Analytical Samples for the Spectroscopic Identification of Molecular Hydrino. CIHT cells having a molten LiOH-LiBr electrolyte and Mo or MoCu alloy anodes served as sources of the theoretically predicted molecular hydrino product $H_2(1/4)$. Magic angle spinning ^1H nuclear magnetic resonance spectroscopy (MAS ^1H NMR), Raman spectroscopy, and photoluminescence emission spectroscopy were performed on reaction products. The molecular hydrino samples comprised CIHT electrodes and the inorganic compound getters KOH-KCl mixture placed in the sealed container of closed CIHT cells wherein hydrinos generated during operation were trapped in the matrix of the compound that thereby served as a molecular hydrino getter. Starting materials not exposed to a hydrino source served as controls.

MAS ^1H NMR. ^1H MAS NMR was performed on solid samples using a 270 MHz instrument with a spin speed of 4.5 kHz. Side bands were eliminated by spinning at two different speeds. Chemical shifts were referenced to external TMS.

Raman Spectroscopy. Raman spectroscopy was performed on solid samples using a Horiba Jobin Yvon LabRAM Aramis Raman spectrometer with a 325 nm HeCd laser that was operated in microscope mode with a magnification of 40X. Additionally, spectra were obtained on MoCu anodes rinsed with deionzed H_2O using a Thermo Scientific DXR SmartRaman

spectrometer having a 780 nm diode laser. The resolution, depending on the instrument focal length, wavelength range, and grating, was typically 1 - 5 cm^{-1}.

Results

CIHT Cell Electrical Energy Balances

As shown in the tables, the electrical energies for CIHT cells comprising hydrogen permeable Mo or MoCu anodes comprising foil membranes continuously output over 48 hour-duration were typically 1.8 times the electrical input at about 10 mW/cm^2 anode area, about a 50 times increase in power density compared to cells of our March report. Using the maximum thermodynamic conversion of 200 kJ/mole H_2 to electricity, the contribution of the permeation hydrogen to the input power was low (<10% of the electrolysis contribution). Using a micrometer it was determined that there was no measureable loss of metal from the hydrogen permeable membrane. The hydrogen protected the anode from corrosion as shown by the comparison with the results of the metal foil anodes. Another benefit was that the cell voltage remained near the open circuit voltage that provided a reduction potential to further stabilize the anode.

The electrical energies continuously output over 48 hour-duration for cells having foil anodes were also typically 1.8 times the electrical input at up to 100 mW/cm^2 anode area. Using a micrometer it was determined that there was measureable loss of metal from the anode. Foil cells at BLP, however, showed metal loss even at much lower power densities. A hydrogen protective effect was clearly observed in the permeation case.

The excess energy in either case cannot be attributed to a metal-air reaction as demonstrated by the results with the substitution of KOH-KBr for LiOH-LiBr. The energy balance was very low despite the metal corrosion being very high.

Spectroscopic Identification of Molecular Hydrino

BLP reported that the CIHT cell getter KOH-KCl showed a shift of the MAS NMR active component of the matrix (KOH) from +4.4 ppm to about -4 to -5 ppm after exposure to the atmosphere inside of the sealed CIHT cell. Enser independently reproduced this result. For example, the MAS NMR spectrum of the initial KOH-KCl (1:1) getter and the same KOH-KCl (1:1) getter from a CIHT cells comprising [MoNi/LiOH-LiBr/NiO] that output about 1.52 Wh, 60 mA, at 179% gain (Figures 1-2) showed that the known downfield peak of OH matrix shifted from about +4 ppm to the upfield region of about -4 ppm.

Using a Thermo Scientific DXR SmartRaman with a 780 nm diode laser in the macro mode, a 40 cm^{-1} broad absorption peak was observed on MoCu hydrogen permeation anodes after the production of excess electricity (Figure 3B). The peak was not observed in the virgin

alloy (Figure 3A), and the peak intensity increased with increasing laser intensity. The absorption peak starting at 1950 cm^{-1} (Figure 3B) matched results of BLP that assigns the peak to an inverse Raman effect from the free rotational energy of $H_2(1/4)$ (0.2414 eV, 1950 cm^{-1}) having a four significant figure match to theoretical predictions.

Another successful confirmatory technique in the search for hydrino product spectra involved the use of the Raman spectrometer. The gas from cell [MoNi/LiOH/NiO] (1.52 Wh, 60 mA, at 179% gain) was gettered with KOH-KCl (50-50 at%), and the Raman spectrum was recorded on the getter using the Horiba Jobin Yvon LabRAM Aramis Raman spectrometer with a HeCd 325 nm laser in microscope mode with a magnification of 40X. In each case, an intense series of 1000 cm^{-1} (0.1234 eV) equal-energy spaced Raman peaks (Figure 4) were observed in the 8000 cm^{-1} to 18,000 cm^{-1} region. The conversion of the Raman spectrum into the fluorescence or photoluminescence spectrum revealed a match to BLP's reported spectra as the second order ro-vibrational spectrum of $H_2(1/4)$[2,3]. The BLP peak assignments to the Q, R, and P branches for the spectra shown in Figure 4 are R(0), R(1), R(2), R(3), R(4), Q(0), P(1), P(2), P(3), P(4), P(5), and P(6) observed at 12,199, 11,207, 10,191, 9141, 8100, 13,183, 14,168, 15,121, 16,064, 16,993, and 17,892 cm^{-1}, respectively.

Practical Considerations

The test cells that were assembled lend themselves to fabrication utilizing more traditional molten salt batteries techniques (i.e. thermal batteries). The electrolyte salt composition is comprised of powdered materials and may be able to be pressed into pellet form utilizing the same high-tonnage pressing techniques that are employed in the thermal battery industry. The anodes and cathodes will take some modification for large-scale production, but there should be no major difficulty in assembling single cell and multi-cell batteries, based on the electrochemistry discussed herein, in a production scale environment. CIHT cell Mo-based anodes can support >100 mW/cm^2 power density from the hydrino reaction without considering the improvement in power density from using high surface area materials versus foil. Since the power contribution from the permeation hydrogen that is capable of protecting the anode is only on the order of a few mW/cm^2, 100 mW/cm^2 excess electricity over permeation is predicted while maintaining anode stability.

Moreover, I confirmed engineering projections that a stack not requiring gas or heat handling systems is feasible wherein a 20 um, porous cathode can support 100 mA/cm^2 from the

[2] R. Mills J. Lotoski, J. Kong, G Chu, J. He, J. Trevey, "High-Power-Density Catalyst Induced Hydrino Transition (CIHT) Electrochemical Cell" (2012).
[3] R. Mills , X Yu, Y. Lu, G Chu, J. He, J. Lotoski, "Catalyst induced hydrino transition (CIHT) electrochemical cell," (2012) submitted.

hydrino reaction with 25 cm diameter plates. Considering the range of surface power densities with dimensions of 10 um, 10 um, and 20um for the anode, the electrolyte layer, and the porous cathode to provide H_2O transport to the reaction, volumetric power densities of 2.5 and 25 kW/liter are feasible having a corresponding material cost of about $70 and $7/kW, respectively.

Conclusion

In summary, Enser scientists and I have successfully fabricated and tested CIHT cells at its facility capable of continuously producing net electrical output of about two times that of the input to maintain the process. The hydrogen permeation successfully stabilized the anode at power densities permissive of multi-kilowatts per liter in a final CIHT cell product. The results indicate that an improvement of at least 10 times this power density appears feasible corresponding to a cost of materials of under $10/kW. The power generation is consistent with Dr. Mills theory of energy release resulting from hydrino formation. No other source of energy could be identified. The predicted molecular hydrino $H_2(1/4)$ was identified as a product of CIHT cells by MAS ^1H NMR, Raman spectroscopy, and photoluminescence emission spectroscopy.

CIHT Cell Electrical Energy Balances

Start Date	Type	Anode description	Initial Thickness (mils)	Final Thickness (mils)	Gain (X)	Cumul Charge (Whr)	Cumul Discharge (Whr)	Net Energy (Whr)	Current (mA)	Charge Step	Discharge Step	V Base @ END (mV)	Typical IR (Ohms)
11/27/2012	HYPR	MoCu 1.5" OD / LiOH+LiBr / NiO	20.5 +/- 0.5	~20 - 25	1.87	0.805	1.502	0.698	50	1s	2s / 0.8V	920	0.28
11/27/2012	HYPR Control	MoCu 1.5" OD / KOH+KBr / NiO	20.5 +/- 0.5	~0 - 34	0.00	1.990	0.001	-1.989	50	1s	2s / 0.8V	Unstable	Unstable
11/28/2012	Flange, Getter	Mo 1 cm^2 / LiOH+LiBr / NiO	41.0 +/- 0.5	~18 - 21	1.79	0.852	1.523	0.671	60	1s	2s / 0.7V	740	0.45
11/28/2012	Open Control	Mo 1 cm^2 / KOH+KBr / NiO	41.0 +/- 0.5	~21 - 38	0.10	0.671	0.064	-0.607	60	1s	2s / 0.7V	Unstable	Unstable
12/3/2012	Open Control	Mo 1 cm^2 on SS Rod / KOH+KBr / NiO	41.0 +/- 0.5	~33	0.29	3.060	0.872	-2.188	60	1s	2s / 0.7V	694	~1

Figure 1. ^{1}H MAS NMR spectrum relative to external TMS of the initial KOH-KCl (1:1) getter that shows the known down-field shifted matrix peak at +4.25 ppm.

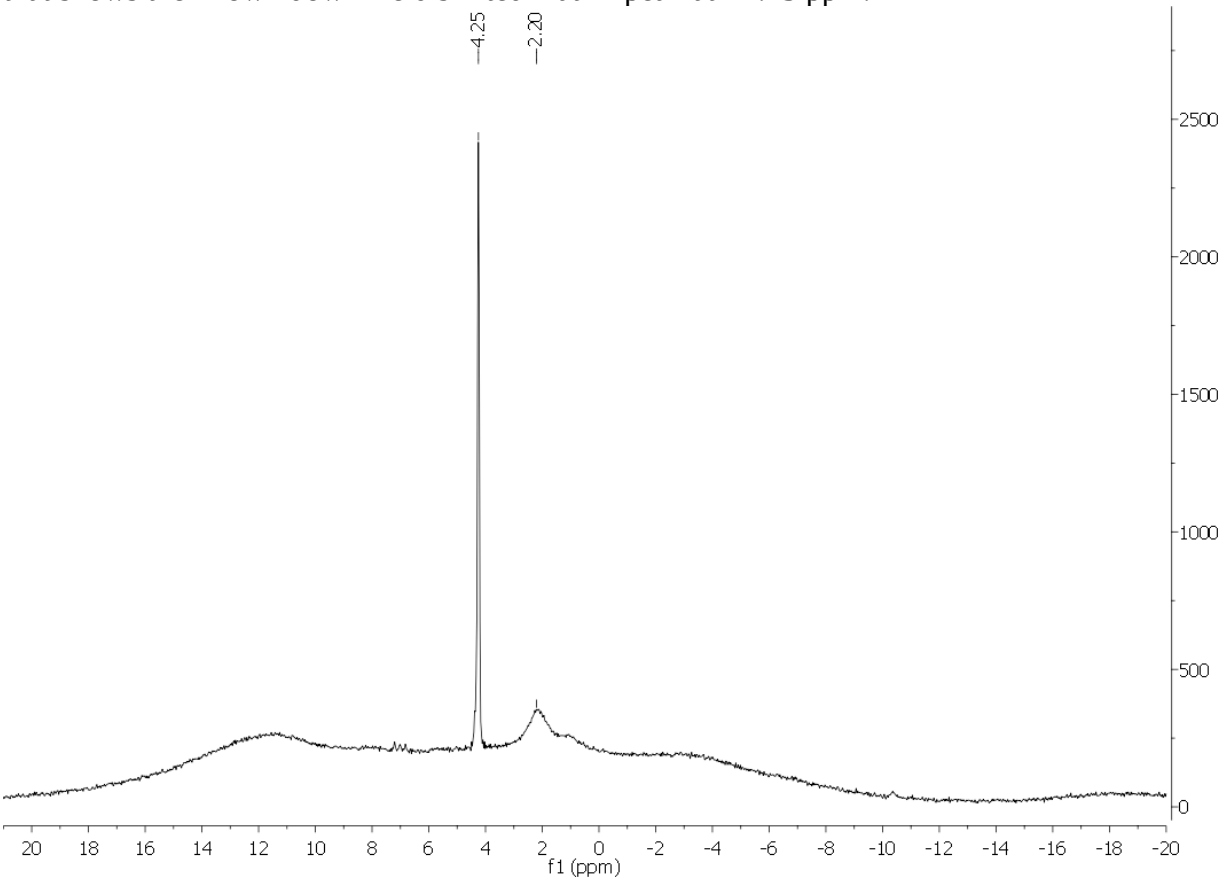

Figure 2. ^{1}H MAS NMR spectrum relative to external TMS of the KOH-KCl (1:1) getter from a CIHT cell comprising [MoNi/LiOH-LiBr/NiO] that output 1.52 Wh, 60 mA, at 179% gain that shows upfield shifted matrix peaks at -4.25 and -4.60 ppm. The symmetrically spaced peaks are spinning side bands.

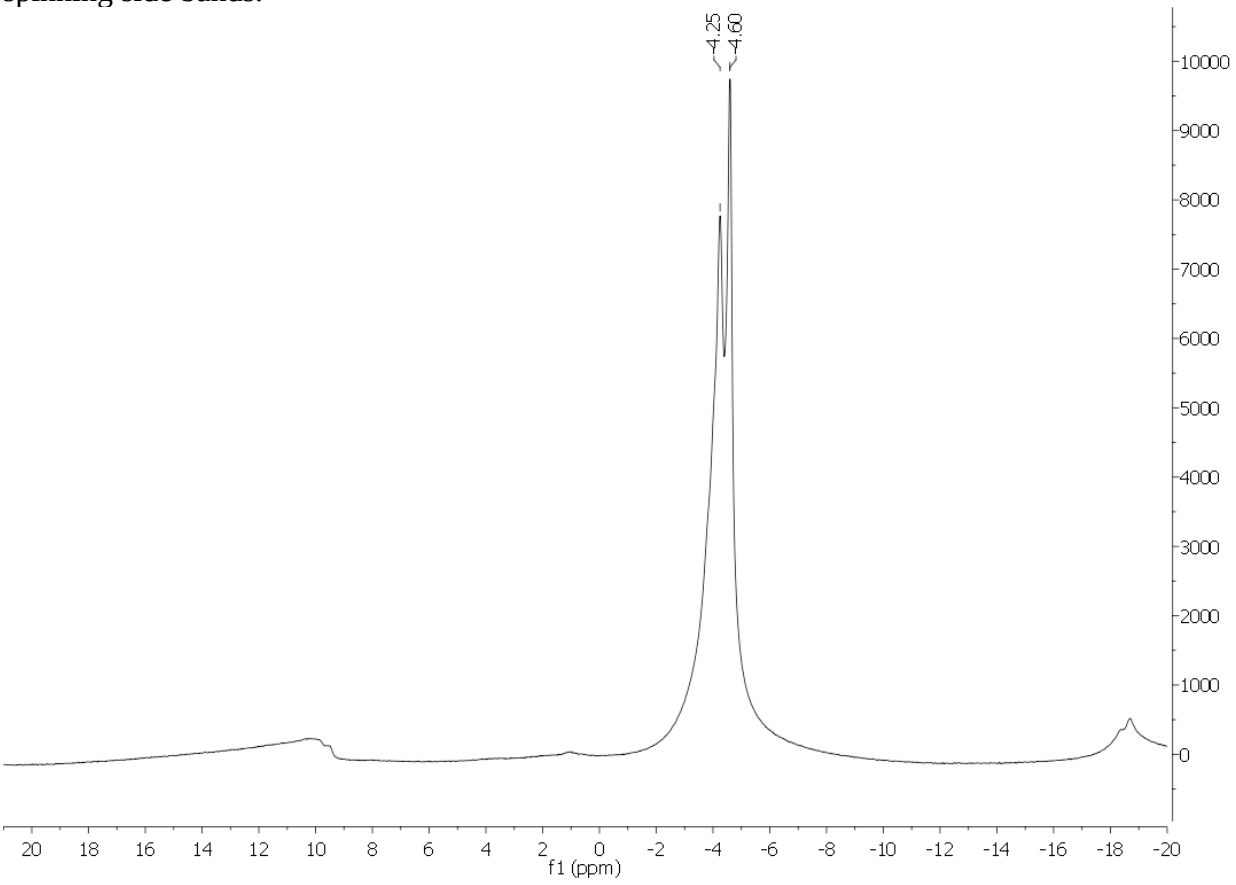

Figures 3A-B. The Raman spectra obtained on MoCu anodes from CIHT cells comprising [MoCu/LiOH-LiBr/NiO] using the Thermo Scientific DXR SmartRaman spectrometer and the 780 nm laser showing a new sharp inverse Raman effect absorption peak starting at 1950 cm^{-1} that matches the free rotor energy of $H_2(1/4)$ (0.2414 eV) to four significant figures. A. MoCu starting material showing no peak. B. Rinsed anode from the CIHT cell [MoCu (H permeation)/LiOH-LiBr/NiO] that output 1.50 Wh, 50 mA, 187% gain.

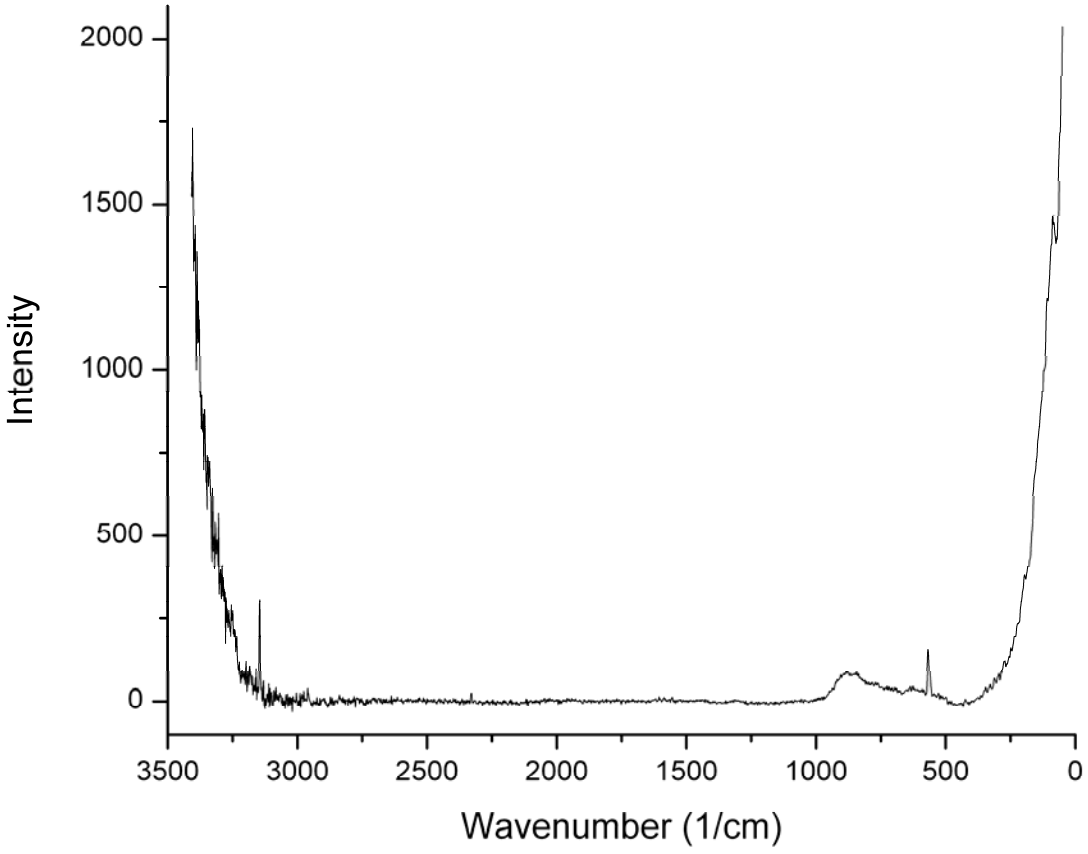

(A)

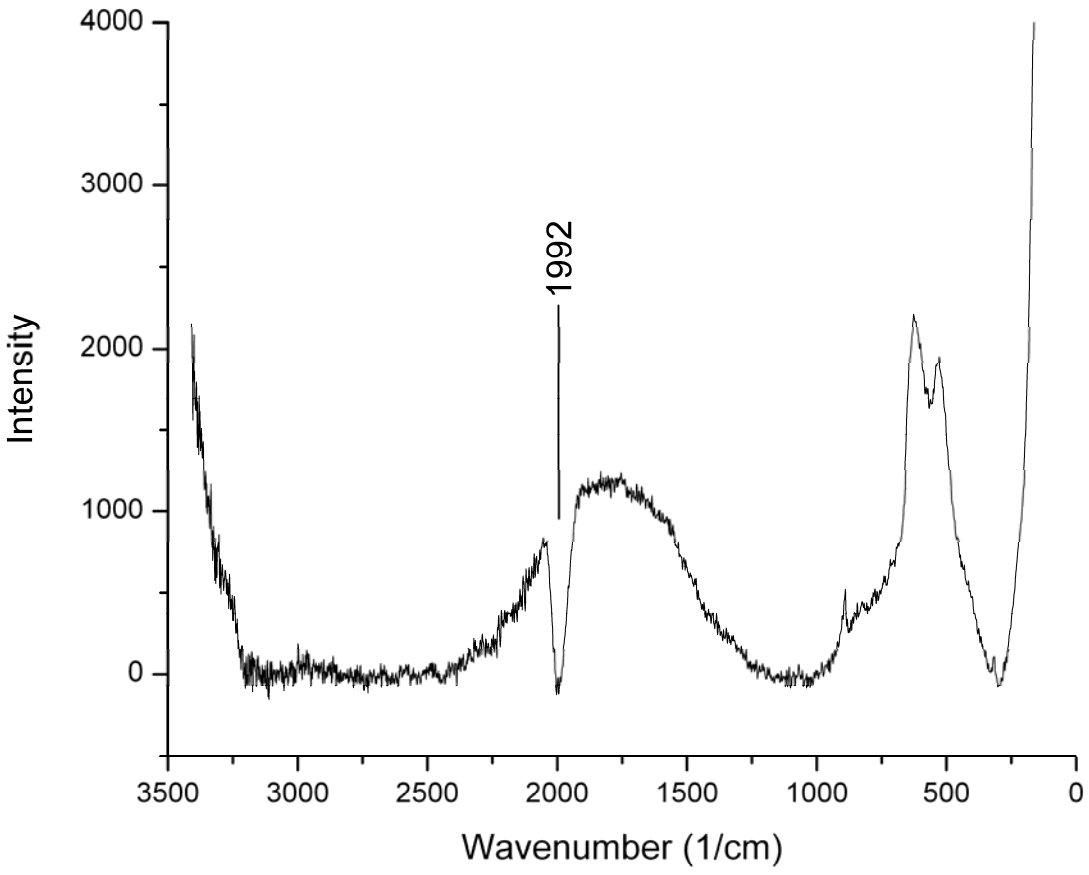
4000
3000
2000
1000
0
Intensity
1992
3500
3000
2500
2000
1500
1000
500
0
Wavenumber (1/cm)

(B)

Figure 4. Raman-mode second-order photoluminescence (PL) spectra of the KOH-KCl (1:1) getter. Bottom trace: Initial KOH-KCl (1:1) getter. Top trace: PL band after exposure to gas from the CIHT cell comprising [MoNi/LiOH-LiBr/NiO] that output 1.52 Wh, 60 mA, at 179% gain.